Hindawi Publishing Corporation
Smart Materials Research
Volume 2013, Article ID 831017, 21 pages
http://dx.doi.org/10.1155/2013/831017

Review Article

MR- and ER-Based Semiactive Engine Mounts: A Review

Mohammad Elahinia,[1] Constantin Ciocanel,[2] The M. Nguyen,[3] and Shuo Wang[4]

[1] *Mechanical Engineering, University of Toledo, Toledo, OH 43606, USA*
[2] *Mechanical Engineering, Northern Arizona University, Flagstaff, AZ 86011, USA*
[3] *Mechanical Engineering, California State University Fresno, Fresno, CA 93740, USA*
[4] *Cinetic DyAG Corporation, 23400 Halsted Road, Farmington Hills, MI 48335, USA*

Correspondence should be addressed to Mohammad Elahinia; mohammad.elahinia@utoledo.edu

Received 9 October 2012; Accepted 7 November 2012

Academic Editor: Mehdi Ahmadian

Hybrid propulsion technologies, including hybrid electric and hydraulic hybrid, equip vehicles with nonconventional power sources (in addition to the internal combustion engine) to provide higher fuel efficiency. However, these technologies tend to lead to higher levels of noise, vibration, and harshness in the vehicles, mainly due to the switching between the multiple power sources involved. In addition, the shocks and vibrations associated with the power sources switching may occur over a wide range of frequencies. It has been proven that passive vibration isolators (e.g., elastomeric and hydraulic mounts) are unable to mitigate or totally isolate such shocks and vibrations. Active mounts, while effective, are more complex, require significant power to operate, and can lead to system instabilities. Semiactive vibration isolators have been shown to be as effective as active mounts while being less complex and requiring less power to operate. This paper presents a review of novel semiactive shock and vibration isolators developed using magnetorheological and electrorheological fluids. These fluids change their yield stress in response to an externally applied magnetic and electric field, respectively. As a result, these fluids allow one to transform a passive hydraulic vibration isolator into a semiactive device.

1. Introduction

In recent decades, the soaring price of fossil fuels has impacted negatively the popularity of the vehicles with internal combustion (IC) engines. This is due, primarily, to the fact that the emissions from IC engines account for a large percentage of the carbon dioxide stored in the atmosphere [1]. In addition, the materials conventionally used for making the cars have become scarcer, and recycling of used cars raised concerns about pollution and waste management. Furthermore, the increasing number of cars worsened the congestion problem and road quality. Among these causes, the gas price and the emission are considered the most important, since they directly affect the wealth of the society and the sustainability of the earth, respectively.

Electric propulsion systems, on the other hand, received more attention as potential candidates for the future of transportation. Nevertheless, since the full electric technology is still in the developing phase and very expensive for regular passenger cars, a great number of modifications to the conventional vehicles have been made in order to achieve higher fuel efficiency and lower emission rate. One of the technologies presented by Kumagai et al. [2] is variable cylinder management which can determine the number of active cylinders of the IC engine based on the driving conditions. For instance, a V6 engine may only need three cylinders, instead of all six, to run the vehicle on the highway. Other common configuration is the hybridization, where the conventional IC engine is coupled with one or more power sources to help reduce the consumed fossil fuel. The additional power sources can be electric or mechanical in nature. The electrical sources often consist of electric motors/generators, batteries, and wires [3], while the mechanical systems may be a flywheel or hydraulic system, the latter including fluid pumps/motors, pressured accumulators, and hoses/pipes.

Hybridizations including both hybrid electric and hydraulic hybrid are structured in one of the two configurations: parallel (mild) or series (full) [4]. In a parallel type,

the vehicles still have the conventional powertrain with the IC engine connected directly to the differential through the driveshaft. The additional power source is also coupled to the driveshaft only to capture the excessive energy of the vehicle. The excessive energy comes primarily from driving downhill or from regenerative braking. In regenerative braking process, when the vehicle wants to slow down, instead of using the brake pads, the electric generator (or hydraulic pump) is engaged with the driveshaft. The torque used to generate the electricity (i.e., stored in a battery), or to pump the fluid from a low pressured reservoir to a high pressured accumulator, reduces the vehicle speed. When the vehicle attempts to accelerate, the electricity from the battery, or the flow from high pressure accumulator to low pressure reservoir, will rotate the driveshaft to move the vehicle forward, instead of the engine. The engine will be turned back on when this stored energy is depleted. In series hybrid vehicles, the driveshaft is totally removed. The IC engine drives a generator (or hydraulic pump), and the created energy (electricity or fluid flow) runs the motor which is integrated to the differential. Beside the benefit of regenerative braking, the series hybrid vehicles have further improved fuel economy than the parallel type because the IC engines are decoupled from the road profile and are allowed to operate at the highest efficiency level. The improvement in fuel economy of a vehicle can reach 70%.

Noise and vibration (NV) are usually generated by the power sources, and they get amplified by the operational modes. In conventional vehicles, the NV issue is associated only with the operation of the internal combustion engine. However, in hybrid vehicles, the NV also comes from the added power sources, that is, the electric generator/motor in a hybrid electric vehicle (HEV) or hydraulic pump/motor in a hydraulic hybrid vehicle (HHV). The operational modes of the modern vehicles make the NV issues even more challenging. A common practice of the advanced vehicular technologies, that adds complexity to the NV problem, is the turning on/off of the power sources [6]. For instance, a regular V6 engine is dynamically balanced when all six cylinders are working. However, in a vehicle with variable cylinder management, when the engine operates with only three cylinders, a considerably large unbalanced force/torque is generated and transferred to the engine mounts. Similarly, in the parallel hybrid vehicles, the unbalance is caused by the engagement of the additional power sources to the driveshaft. In addition, hybrid vehicles experience a lot of switches between the power sources at high rotational speed (rpm), or torque, during their operation. As a result, shock loads are induced at variable amplitudes. The operating characteristics of the additional power sources also extend the range of vibration frequency. As an example, the hydraulic pump shows large harmonics between 200 and 250 Hz while working at 1500 rpm.

Over the past decades, magnetorheological (MR) fluids and electrorheological (ER) fluids have been implemented in many vibration-related engineering applications due to their unique properties. MR fluids are made of micron-sized iron particles that are suspended in a carrier liquid such as mineral oil, synthetic oil, water, or glycol [7]. ER fluids are suspensions of nonconducting microparticles in an electrically insulating fluid. The apparent viscosity of these fluids changes reversibly by an order of up to 100,000 in response to a magnetic and an electric field, respectively.

MR and ER fluids can operate in flow, shear, and squeeze modes. In flow mode, the magnetic poles/electrode plates are fixed, making this mode suitable for hydraulic controls, servovalves, dampers, and shock absorbers. The shear mode, with a pole/electrode plate moving parallel to the other, is suitable for clutches and brakes, chucking/locking devices, dampers, breakaway devices, and structural composites. The squeeze mode, with the two magnetic poles/electrode plates moving toward each other, could be considered for small amplitude vibration and impact dampers. Because of the fluids' millisecond response time, MR and ER fluid-based devices are capable of working in a wide frequency range from zero to a few hundred hertz.

The focus of this paper is on MR and ER fluid-based mounts developed for vibration mitigation in a wide variety of applications. An MR/ER fluid-based mount is constructed very similarly to a hydraulic mount and consists of multiple components. The key parts of the mount are the top and bottom rubber, top and bottom fluid chambers, flow passages, and an MR or ER fluid. In this paper, the literature presenting MR and ER engine mounts is reviewed. The knowledge from this review is desired to be a starting point for future semiactive/active engine mounts.

2. Magnetorheological Fluid Mounts

The idea of using MR fluids for vibration mitigation applications was first proposed by Carlson [8], and the first reported implementation of ME fluids in mounts was made by Ahn et al. [5]. At the time, the authors proposed the usage of MR fluid in the inertia track of a conventional hydraulic mount for the purpose of controlling the flow through the inertia track, that is, between the two chambers of the mount. Essentially, the MR fluid has been used in this implementation as a valve, to close or open the inertia track. The schematic of the proposed implementation is shown in Figure 1 in comparison with the traditional mount.

Replacing the hydraulic fluid inside the mount with MR fluid improves its vibration isolation capabilities. The effect of the MR fluid is the most beneficial at frequencies higher than the notch frequency of the mount. When the MR fluid is activated inside the mount, it acts like a valve and facilitates the control of the fluid flow through the inertia track of the mount. Controlling the fluid flow through the inertia track eliminates the peak in mount's transmissibility as shown in Figure 2. In addition, the dynamic stiffness of the mount can be controlled with an outcome as that shown in Figure 3. Overall, the substitution of the hydraulic fluid with the MR fluid, and the implementation of the MR valve, lead to an increase in the overall efficiency of the mount.

Ay et al. [9] converted a hydraulic mount into a semi-active mount by replacing the hydraulic fluid with an MR fluid 132LD developed by Lord Corporation. The fluid's maximum achievable yield stress was 54 kPa at a magnetic

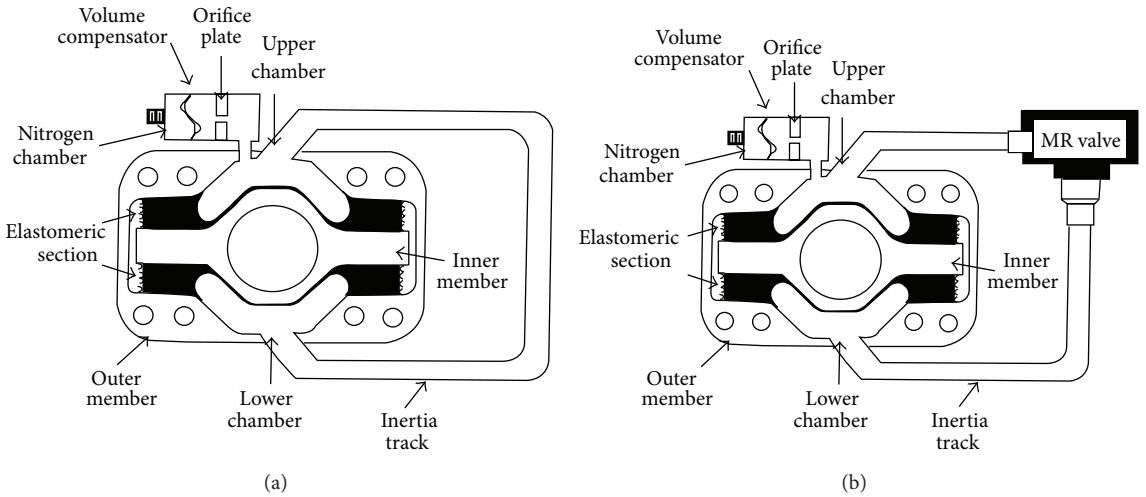

FIGURE 1: (a) Hydraulic mount with external inertia track; (b) MR fluid-based hydraulic mount with MR valve installed along the external inertia track by Ahn et al. [5].

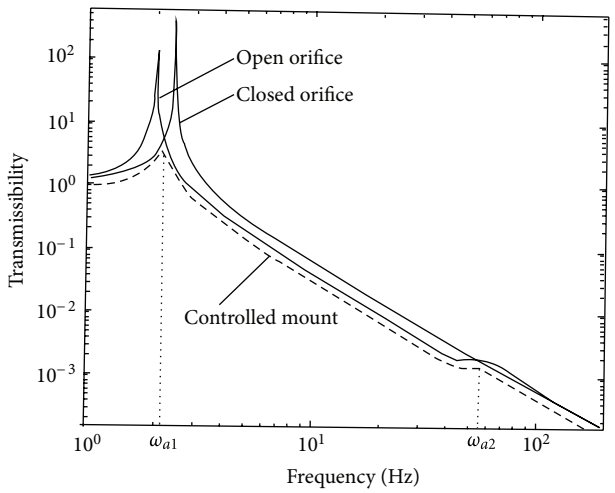

FIGURE 2: The transmissibility of the mount with the MR fluid valve open and closed. The dotted line shows the achievable transmissibility through opening and closing of the MR fluid valve by Ahn et al. [5].

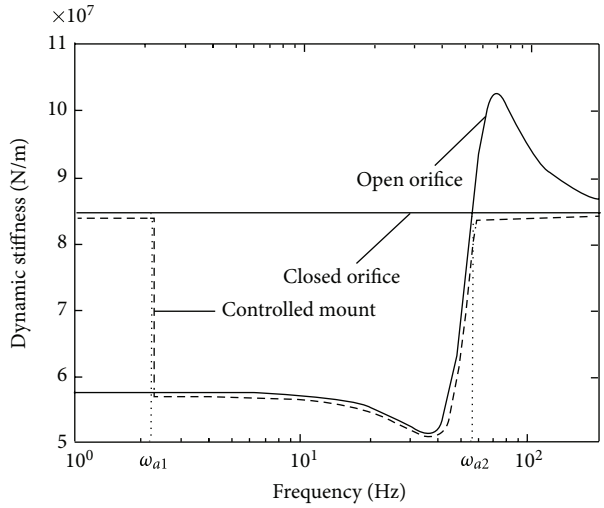

FIGURE 3: The dynamic stiffness of the fluid mount can be controlled through opening and closing of the MR fluid valve by Ahn et al. [5].

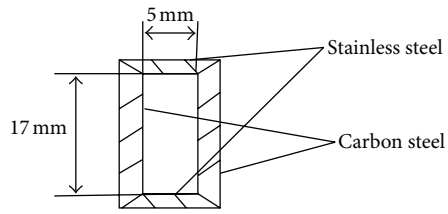

FIGURE 4: MR fluid valve by Ay et al. [9].

field of 1.2 tesla. The approach taken by the group was similar to that of Ahn et al. [5, 10] but applied to a different type of hydromount. The group described in detail the configuration of the MR valve designed to control the fluid flow between the two chambers of the mount indicating that the valve casing had to be made in part of stainless steel and in part of low carbon steel, as shown in Figure 4. This material combination is recommended to insure that the magnetic field flux lines close through the fluid and not through the casing, as it is indicated in Figure 5. A schematic of the mount model is shown in Figure 6 indicating that the mount, in the absence of a feedback system, is very similar to an external tunable damper.

The group performed experiments to identify whether or not the variation of the magnetic field strength could lead to a shift in the frequency response of the mount. These tests were carried out at frequencies of up to 22 Hz with both accumulators pressurized at 34 psi for an operating point

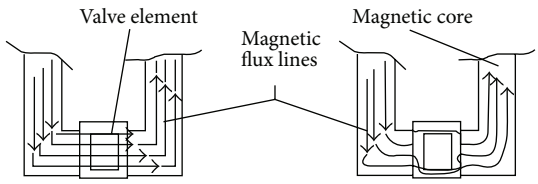

Figure 5: The distribution of the magnetic flux lines through the MR fluid valve made of (a) stainless steel and (b) low carbon steel by Ay et al. [9].

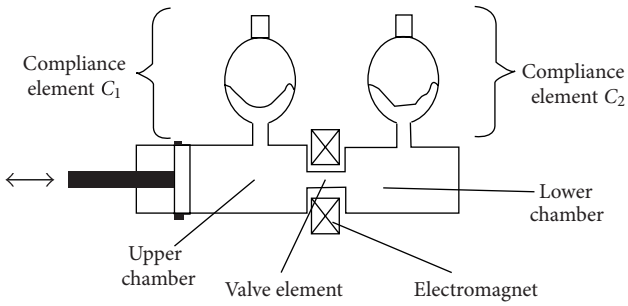

Figure 6: Schematic of the proposed MR mount by Ay et al. [9].

of 41 psi. During these tests, the focus was on the evolution of the pressure values within accumulators 1 and 2 as a function of the applied current over the coil surrounding the MR valve. Figure 7 shows the evolution of pressure in accumulator 1 as a function of the applied current and the frequency of excitation. The results shown in Figures 7 and 8 do not illustrate the expected shift in the resonance frequency of the mount with the applied current, particularly as the resonant frequency of the mount is higher than 22 Hz. However, the pressure evolution in both accumulators as a function of the applied current indicates that a change in mount stiffness does occur as the valve further restricts the flow with the increase in the applied current. This suggests that the use of MR fluid could benefit the overall response of the mount.

Ahn et al. [10] developed an MR fluid-based mount to be used for supporting electronic equipment (e.g., CD players) inside automobiles. The schematic of this mount is shown in Figure 9. The results presented by the authors indicate that the MR fluid addition to the mount reduces the peak transmissibility about three times, in addition to shifting the peak in transmissibility by about 4 Hz toward higher frequencies.

However, from the body of the paper it is somewhat vague whether the results shown in Figure 10 are theoretical/simulated or experimental; the text does imply that the numerical results match the experimental ones when the volumetric stiffness and damping of the MR mount are 6 and 9 times, respectively, higher than those of a regular hydraulic mount with the same configuration. These results are very encouraging and prove the potential of MR fluids for

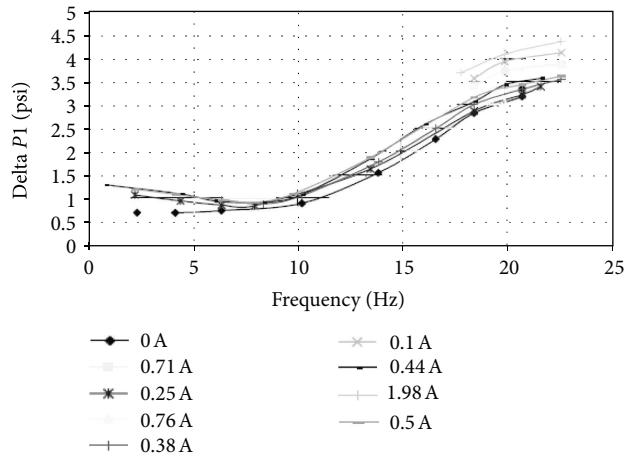

Figure 7: Evolution of the pressure in accumulator 1 as a function of the applied current and frequency of excitation by Ay et al. [9].

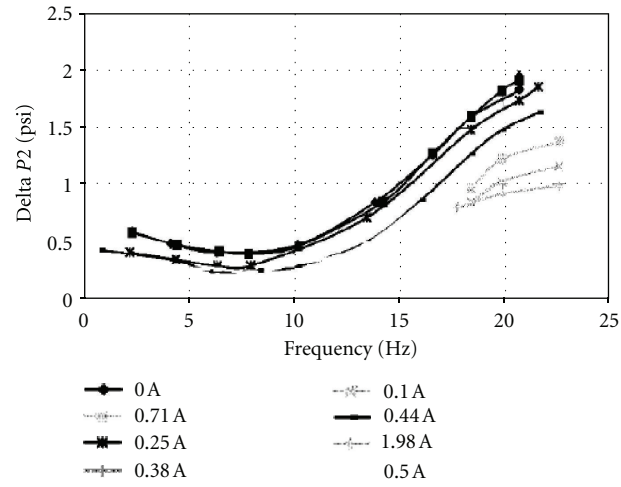

Figure 8: Evolution of the pressure in accumulator 1 as a function of the applied current and frequency of excitation by Ay et al. [9].

transforming hydraulic mounts from a passive to an active system.

Hong and Choi [11] developed a flow mode MR fluid-based mount whose schematic is shown in Figure 11. The critical dimensions identified in Figure 11 are piston radius $r = 8.5$ mm, gap size $h = 1.5$ mm, and gap length $L = 10$ mm. These dimensions were selected based on the desired damping force for the mount and the yield stress of the MR fluid used (i.e., MRF 132LD).

The configuration proposed by the authors resembles that of an MR fluid-based damper, and, as such, the main characteristic affected by the presence of the MR fluid is the damping, which can be controlled through the current applied to the coils inside the mount. Figure 12 shows the evolution of the damping force with the applied current, indicating that the damping force increases with the current increase.

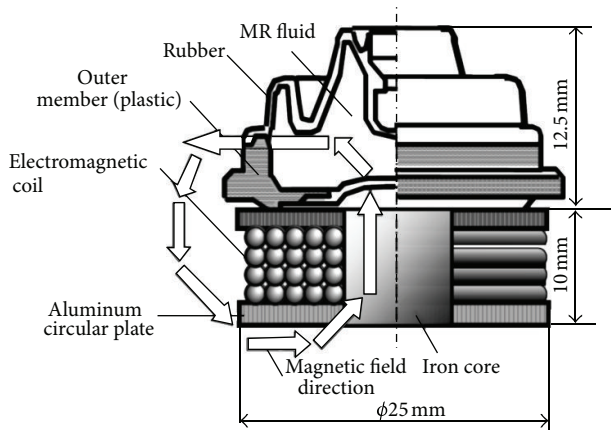

FIGURE 9: An MR fluid mount for electronic equipment isolation inside a car by Ahn et al. [10].

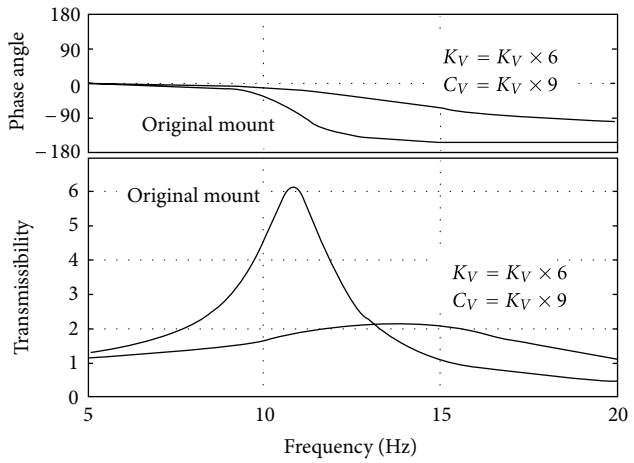

FIGURE 10: Transmissibility and phase angle for the MR mount with variable damping and stiffness by Ahn et al. [10].

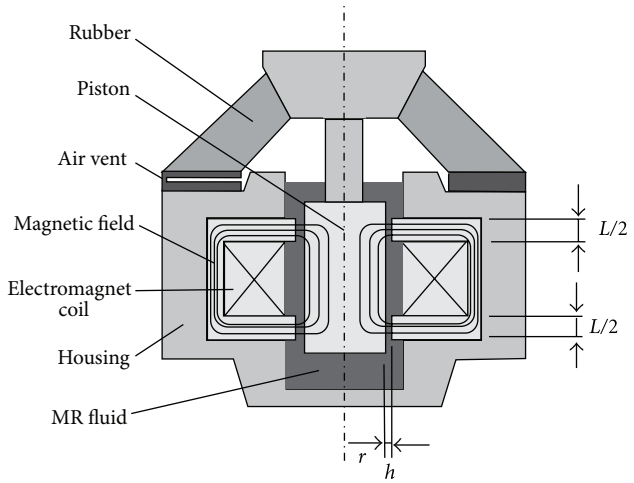

FIGURE 11: Schematic of a flow mode MR mount by Hong and Choi [11].

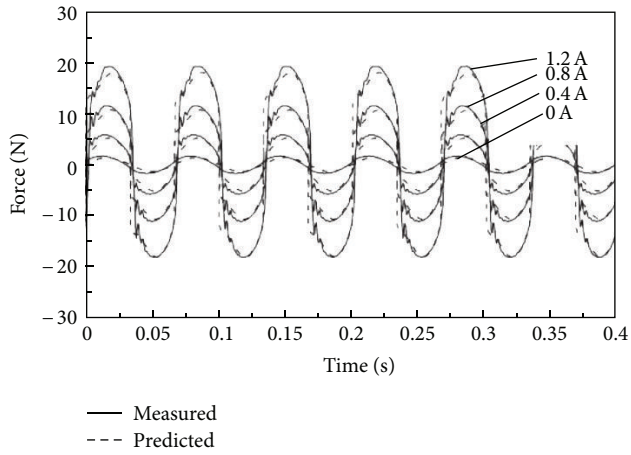

FIGURE 12: Simulated and experimental values of the damping force as a function of current by Hong and Choi [11].

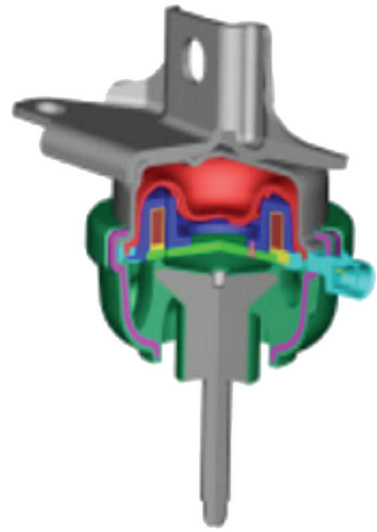

FIGURE 13: Delphi's power train MR mount by Delphi Corp. [12].

Delphi Corporation [12] released an MR fluid-based pow-ertrain mount and provided, in a brief technical note, the characteristics of the mount and a nonenabling representation of their mount. The mount configuration is shown in Figure 13 and the damping and dynamic stiffness characteristics of the mount are shown in Figure 14. While the mount appears to be able to operate at electric currents as high as 5 A, the trend in damping and dynamic stiffness curves suggests that the operation up to 1 A is most desirable. Applying currents above 1 A leads to a significant drop in damping and an increase in dynamic stiffness; this may be due to the freezing of the MR fluid inside the mount. This mount was designed to control the engine's torque transient response to the coupling and shifting of gears.

Barber and Carlson [13] designed and tested two engine mounts filled with LORD Glycol MR fluids containing 22 and 36 percent of iron per volume. One mount had inertia track

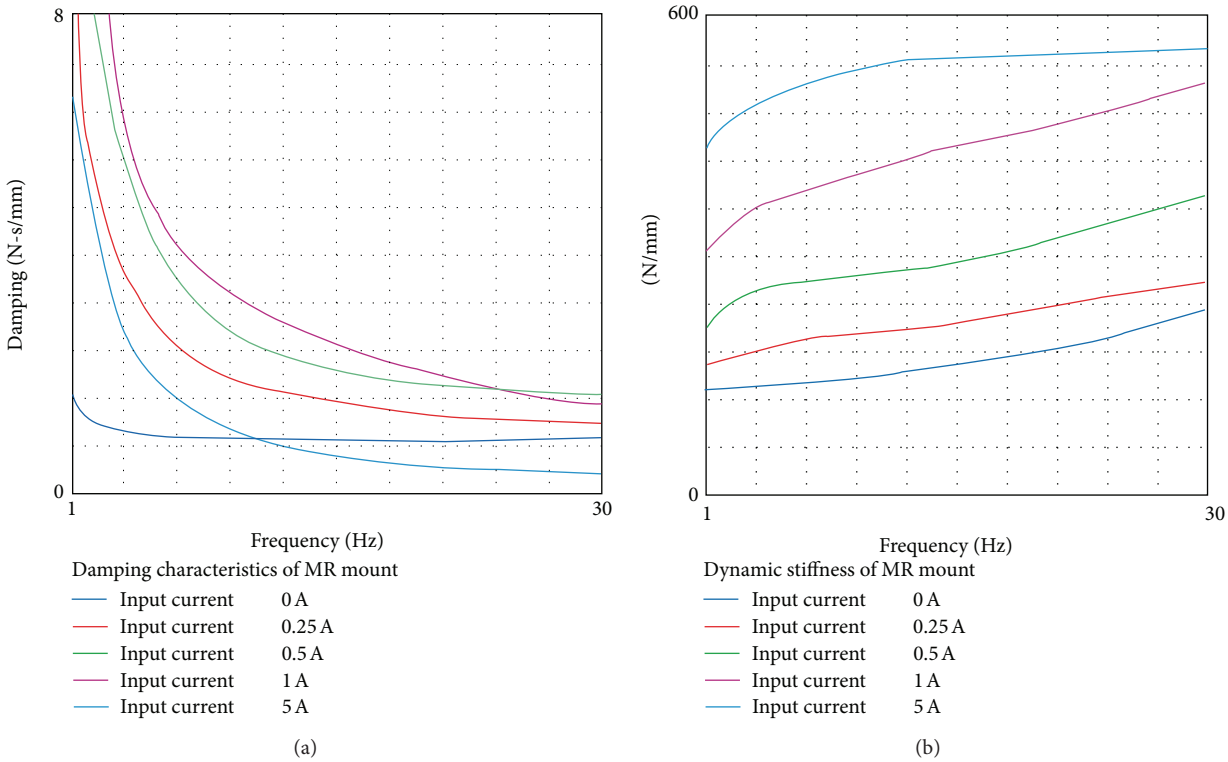

Figure 14: Damping characteristic of the Delphi MR mount (a); dynamic stiffness characteristic of the Delphi MR mount (b) by Delphi Corp. [12].

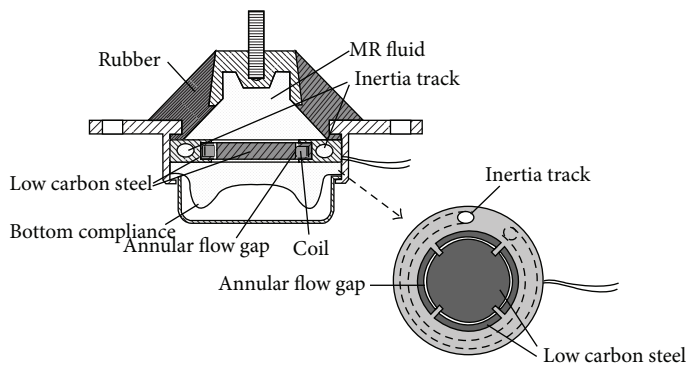

Figure 15: MR mount developed by Barber and Carlson [13].

and a flow valve, while the other had only a flow valve. The latter was tested only with MR fluid containing 22% of iron per volume. A schematic of the mount with inertia track and flow valve is shown in Figure 15. The mounts were tested at 0.1 mm and 1 mm displacements, in the frequency range of 1 to 25 Hz, under several magnetic field amplitudes.

The dynamic stiffness for the MR valve mount exhibits a mild increase with the increase in frequency (see Figure 16), while for the MR mount with inertia track the dynamic stiffness first decreases leading to a notch frequency around 5 Hz, then increases continuously for excitation currents of 1 A (see Figure 17). At 2 A excitation current, the dynamic stiffness increases suddenly after the notch frequency and holds that level up to about 15 Hz; after that a decrease in stiffness occurs. At 3 A excitation current, after a sudden increase in dynamic stiffness after the notch frequency, the dynamic stiffness drops continuously, exhibiting a dip around 15 Hz.

Nonetheless, these results indicate the feasibility of controlling the dynamic stiffness of a mount by means of changing the magnetic field to which the MR fluid is exposed within the valve and/or inertia track. This is confirmed by the results presented in Figure 18 that compare the dynamic stiffness of a regular hydraulic mount with that of an MR fluid-based mount.

Another design approach, shown in Figure 19, was taken by Mansour et al. [14]. The authors incorporated an MR chamber, that is the equivalent of an MR damper, into the

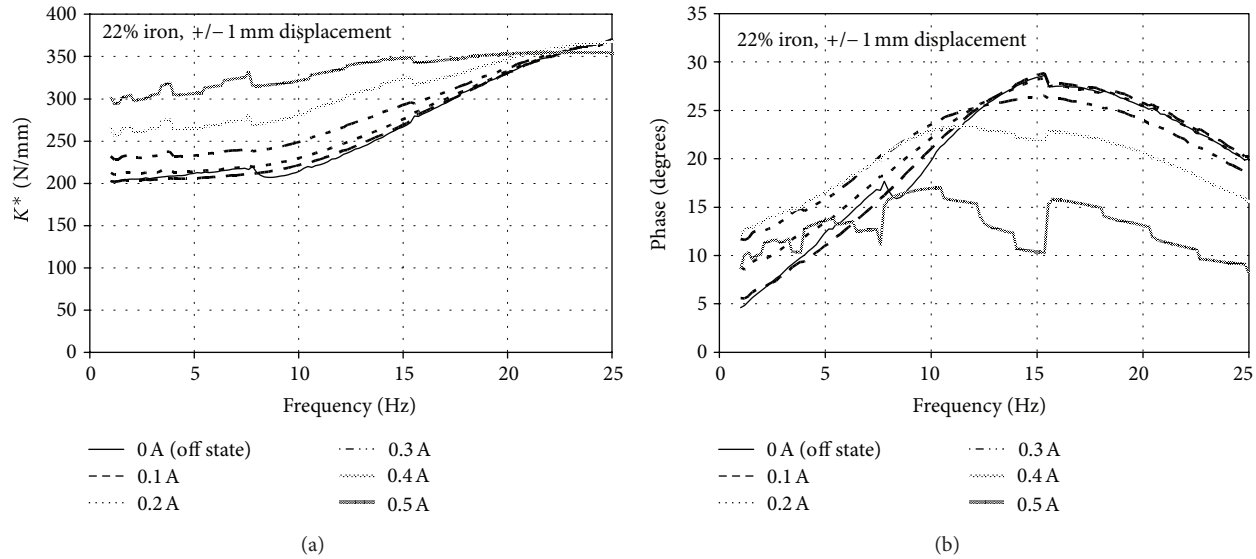

FIGURE 16: Results for dynamic stiffness (a) and phase angle (b) for the mount with MR valve only. The excitation was 2 mm peak to peak and the currents applied to the coil were varied between 0 and 0.5 A in 0.1 A increments by Barber and Carlson [13].

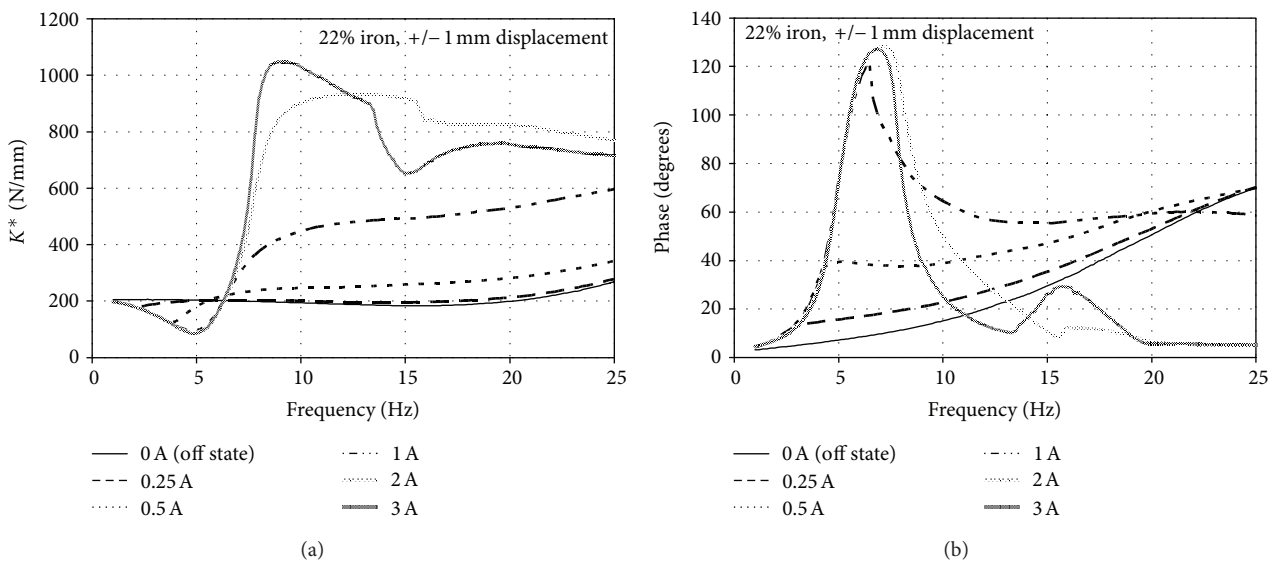

FIGURE 17: Results for dynamic stiffness (a) and phase angle (b) for the mount with MR valve and inertia track. The excitation was 2 mm peak to peak and the currents applied to the coil were varied between 0 and 3.0 in several increments by Barber and Carlson [13].

top chamber of a hydraulic mount. The chamber, shown in Figure 20, facilitates the control of the compliance of the upper chamber of the mount. Numerical simulations results shown in Figure 21 indicate that an increase in compliance of the top/pumping chamber of the mount (denoted by C_1 in the figure) leads to a decrease in dynamic stiffness of the mount. Accordingly, the MR chamber was added to facilitate the control of the dynamic stiffness by controlling the upper chamber compliance. The dynamic stiffness and phase angle of the mount, with the MR chamber activated at different levels of magnetic field, is shown in Figure 22.

An MR mount combining the valve mode and squeeze mode was proposed by Nguyen et al. [15]. The structure of the mount is presented in Figure 23.

The main components of the mount are numbered in this figure as follows: (1) upper rubber part, (2) bottom rubber part, (3) inner coil, (4) inner coil housing, (5) outer coil, (6) outer coil housing, (7) flow passage, (8) mount housing, (9) closing ring, (10) upper mounting connecting rod, (11) upper squeeze plate, and (12) lower mounting connecting rod. The middle assembly, that is, components 3 through 6, separates the inner volume of the mount into two chambers.

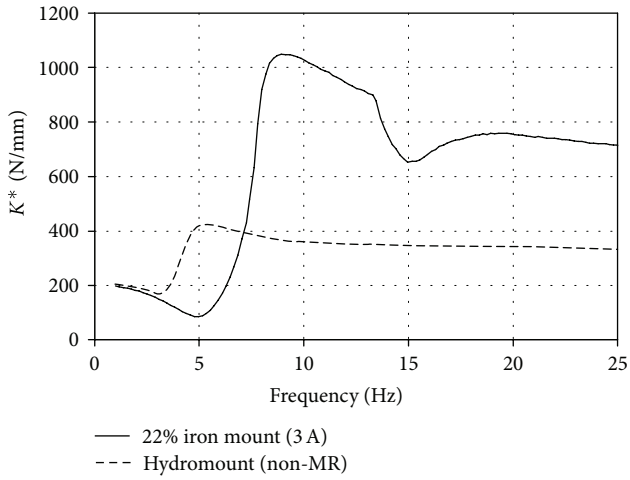

FIGURE 18: Comparison between the dynamic stiffness of a hydraulic mount and that of the MR mount by Barber and Carlson [13].

FIGURE 19: MR fluid-based mount developed by Mansour et al. [14].

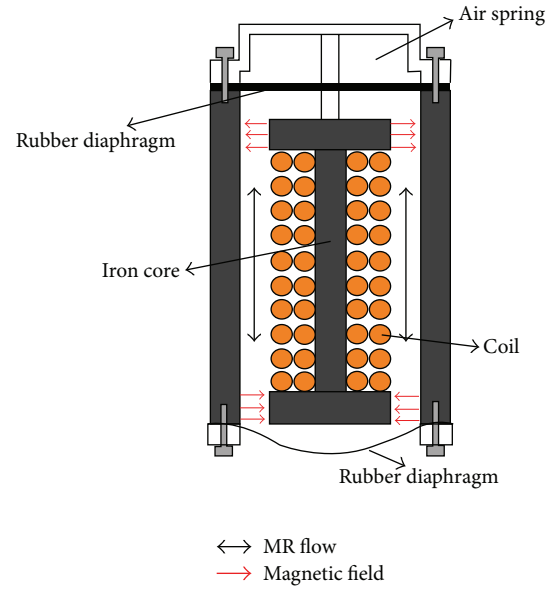

FIGURE 20: MR chamber embedded in the mount shown in Figure 19 by Mansour et al. [14].

The upper chamber is enclosed by the top rubber (1). The lower chamber is enclosed by the bottom rubber (2). The MR fluid, not shown in Figure 3, flows between the upper and lower chambers via flow passages (7) located within the middle assembly. The housing is comprised of part (8) and the closing collar (9). The mount is assembled by tightening the collar against the housing with eights screws (not shown in Figure 23). The upper rubber part has to support the static load applied to the mount (i.e., the engine block), while the bottom rubber is necessary to contain the MR fluid. Accordingly, the upper rubber has very low compliance while the bottom rubber has very high compliance. However, the upper rubber part is configured such that, despite of its low compliance, it bulges when the fluid does not flow through the flow channel and/or the mount squeeze mode plates are not touching. The inner coil (3) provides the magnetic field that activates the squeeze mode, while the outer coil (5) generates the field that activates the flow mode. The inner and outer coils are enclosed in housing, (4) and (6), made of 1018 high magnetic permeability steel.

The top rubber is molded around screw (10) that serves two purposes in this design: to attach the mount to the supported mass (the engine) and to support the plate (11). The bottom surface of the plate (11) and the top surface of the housing (4) are the surfaces between which squeezing of the MR fluid happens during mount operation. The parts shown in grey and silver colors in Figure 23 are made of nonmagnetic materials.

The experimentally determined dynamic stiffness of the mount at 0.4 mm amplitude of excitation, in flow/valve mode, squeeze mode, and in the combined flow-squeeze modes varies as shown in Figure 24. This figure indicates the range over which the dynamic stiffness can be controlled during the operation of the mount. The mixed mode mount

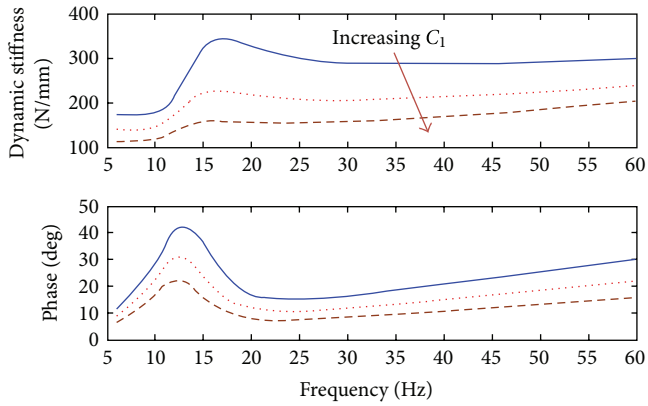

FIGURE 21: Simulated results for the change in dynamic stiffness and phase angle of the mount with the change in magnitude of compliance of the upper chamber of the mount by Mansour et al. [14].

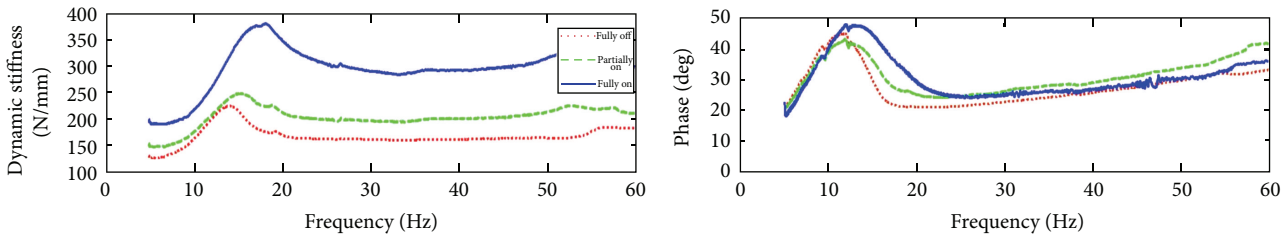

FIGURE 22: Experimental values for the dynamic stiffness characteristic (a) and phase angle (b) of the MR fluid-based mount developed by Mansour et al. [14].

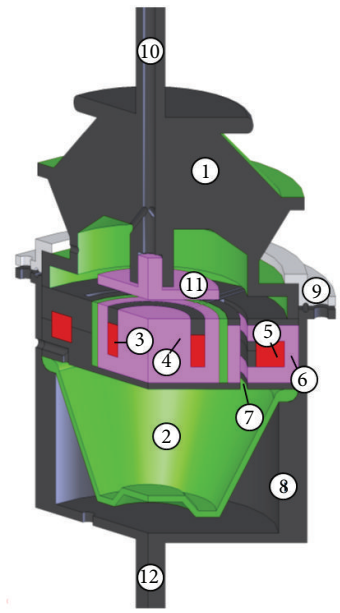

FIGURE 23: Section view of the MR mount by Nguyen et al. [15].

expands significantly the amplitude margins (between the notch and peak) of a passive hydraulic mount. The dynamic stiffness envelope is very large which allows the users to have a desired stiffness at any frequency. Besides, the ability to set the dynamic stiffness for any excitation amplitude optimizes the vibration isolation process.

3. Electrorheological (ER) Fluid-Based Mounts

ER fluid mounts can be divided into three categories: (a) flow mode, (b) squeeze mode, and (c) flow and shear mode. The following paragraphs describe the layout and performance of these types of mounts.

3.1. Flow Mode. The flow mode ER mount, shown in Figure 25, proposed by Hong et al. [16] was designed to support a high static load of 200 kg. Its structure is similar to that of a regular hydraulic mount, having upper and lower fluid filled chambers connected via an inertia track. In this mount, the inertia track was replaced by the concentric annular flow passages. The concentric rings, which separate the flow passages, act as electrodes when the mount is powered with an electric potential. Therefore the fluid flow through these passages is controlled by varying the electric field between these electrodes. The flow control, in turn, affects the damping of the mount.

The mount was tested between 0 and 30 Hz with several input displacement amplitude levels. Without a control

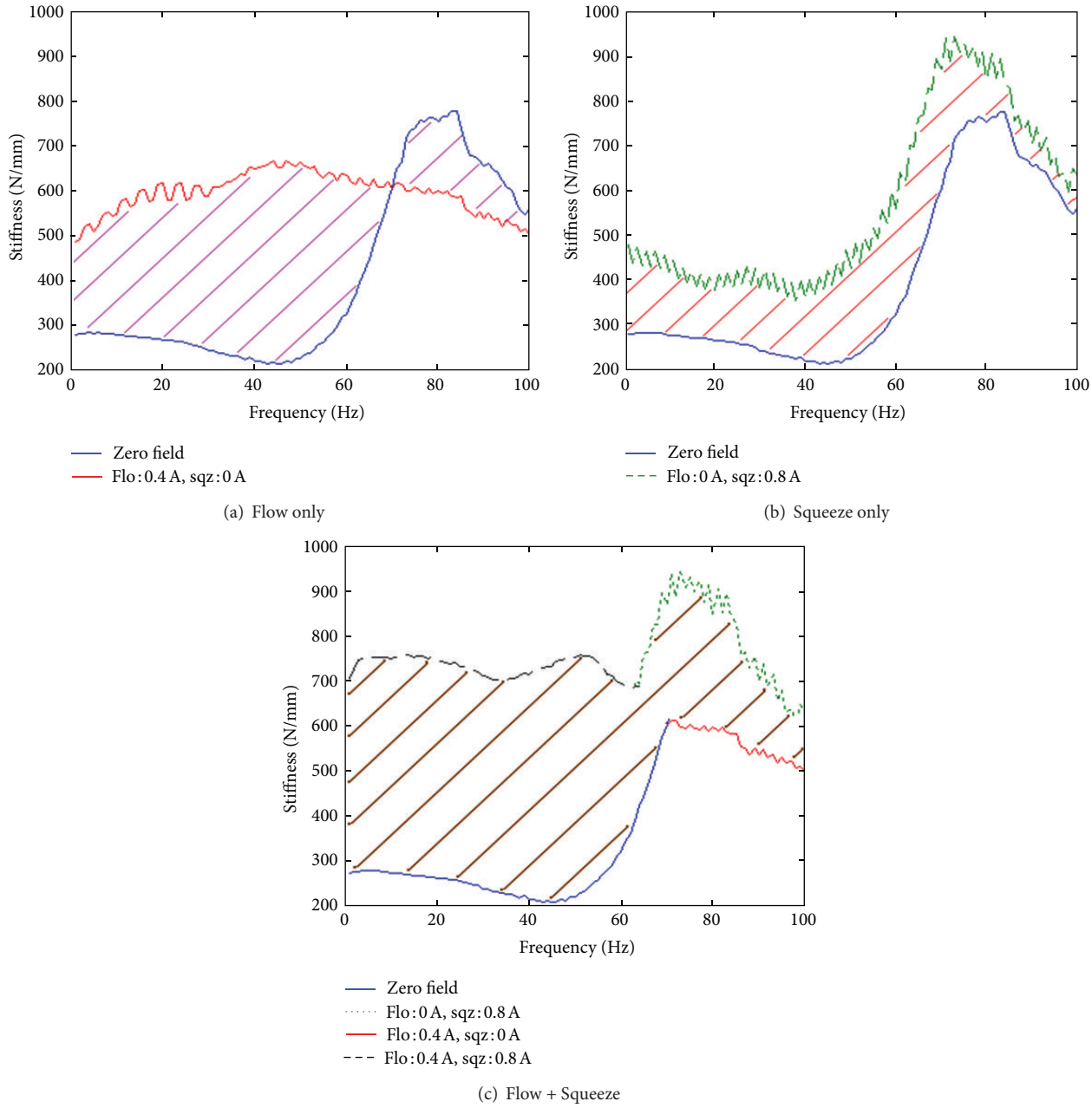

FIGURE 24: Comparison in performance of individual modes and combined mode at 0.4 mm displacement by Nguyen et al. [15].

strategy implemented (i.e., passive modes), the ER mount performance did not vary significantly, even at largely different electric fields. With a skyhook control algorithm, the ER mount leads to a significant reduction in transmissibility. However, the shift in frequency between the on and off state was very small, that is, only 1-2 Hz.

3.2. Squeeze Mode. For the squeeze mode, the ER mounts by the group of Stanway in Figure 26 [17–20] and the group of Hong in Figure 27 [16, 21] have many features in common. They both support the static load by a coil spring; the two steel discs, that is, electrodes, are separated by the volume of ER fluid; the upper disc moves with the supported mass while the lower disc is moving with the base. When the mount is squeezed or extended, the ER fluid flows out or in, respectively. These two mounts are effective in reducing the transmissibility. However, the mounts do not have the capability of shifting the resonant frequency.

The squeeze mode ER mount by Hong et al. [22] (Figure 28) was configured slightly different from the ones in Figures 26 and 27. Its lower structure is similar to that of the mount by Hong et al. [16], but the upper structure resembles the flow mode ER mount by Hong et al. [22] which has the top rubber of a regular hydraulic engine mount.

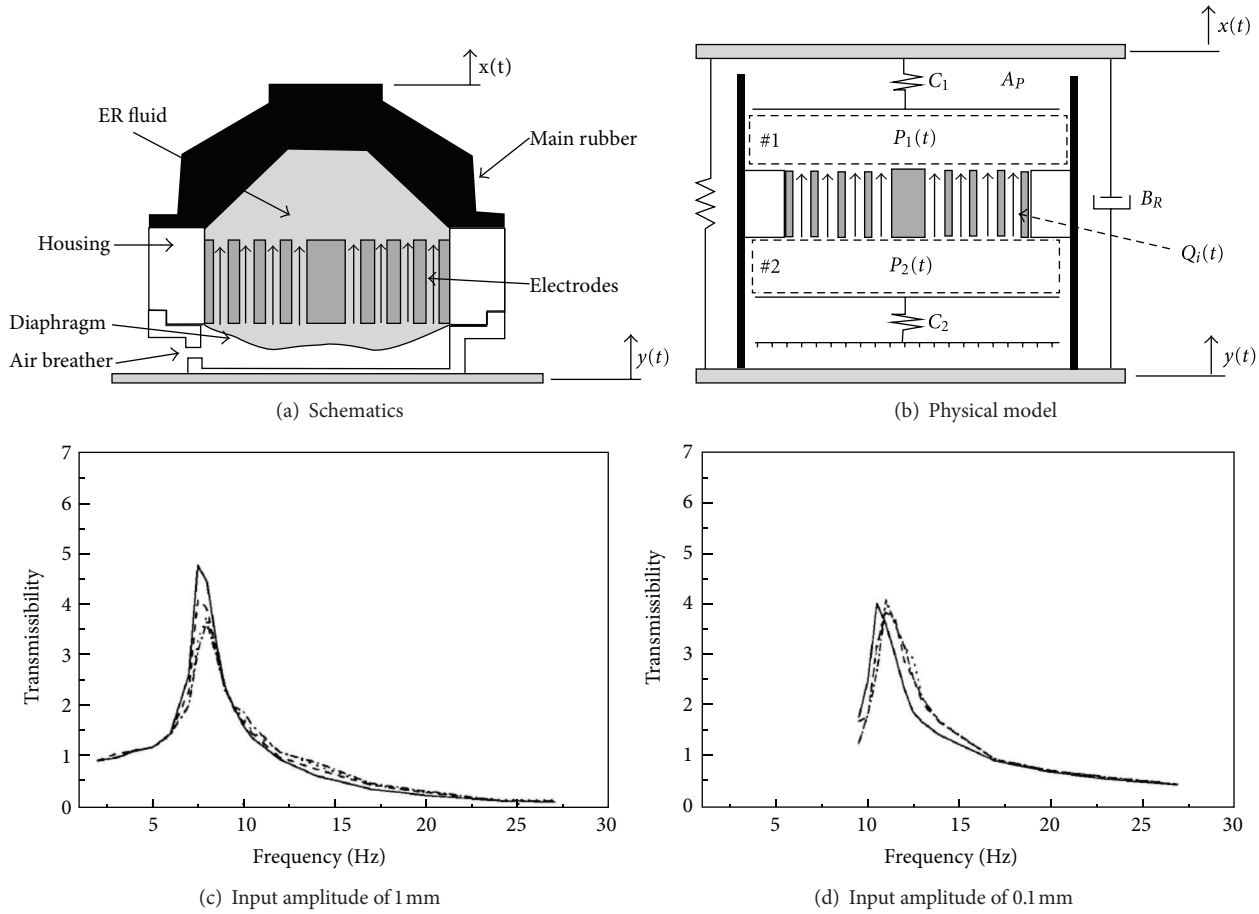

Figure 25: Flow mode ER mount by Hong et al. [16].

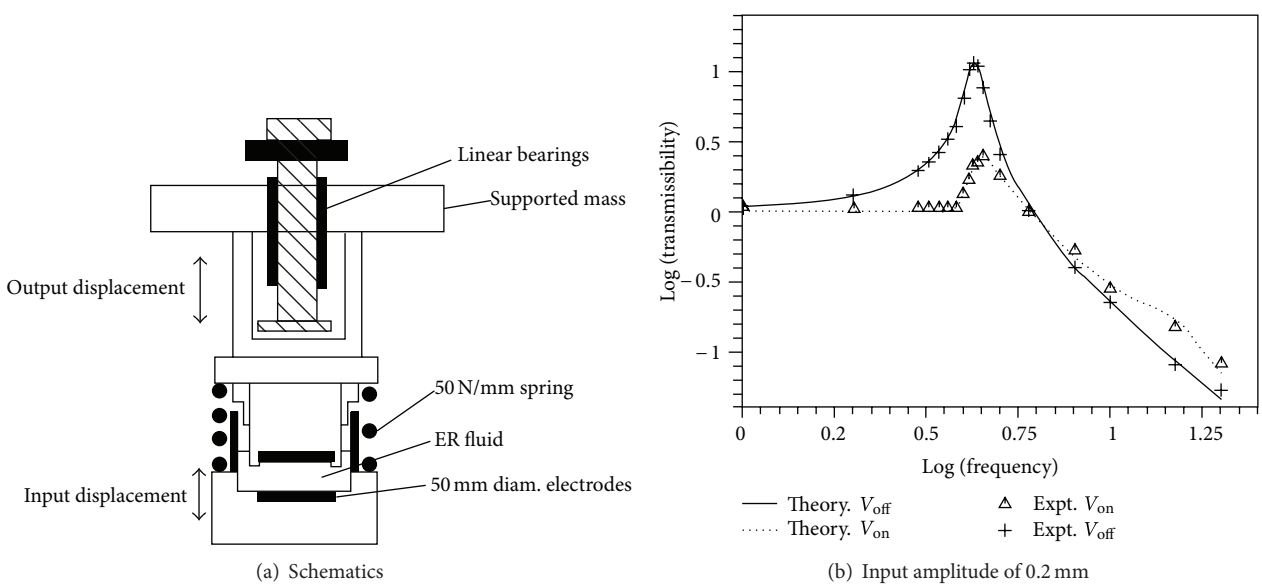

Figure 26: (a) ER engine mount investigated by the Stanway group [17] and (b) theoretical and experimental changes in the transmissibility of the mount, in on and off states, [18].

This squeeze mode ER mount experienced a wider shift in resonant frequency, about 5 Hz, between the off and the on state (at the highest electric field state), and performed similar to other ER mounts in transmissibility amplitude reduction.

3.3. Mixed Mode: Flow + Shear. The mixed mode ER mounts by Choi et al. [23], Figure 29, and Choi and Song [24], Figure 30, are very similar in design. The only difference is that the earlier one supports the mass by the coil spring, while the latter one uses the top rubber of a regular hydraulic engine mount. The mounts are expected to function in two modes: flow and shear. The flow mode happens due to the change in volume of the upper and lower chambers when the top vibrates, while the shear mode occurs as one set of the electrodes is moving with respect to the other set.

Similarly to other ER mounts, these two mounts can provide low transmissibility, but with a very small shift in resonant frequency, about 2-3 Hz.

The ER mount shown in Figure 31 by Lim et al. [25] was not designed for car engine. It was to be used for controlling the shock and vibration of a CD-ROM. Therefore, it has very small size and simpler inner structure. The inner electrode is attached to the top rubber which supports the feeding system including the motor and the optical. The outer electrode is fixed with the base where the external shock and vibration happen. Similar to other mixed mode ER mounts, Figures 29 and 30, the flow mode happens between the upper chamber and the shear mode takes place between the electrodes.

Since this ER mount was for mitigating the CD-ROM vibration problem, the tested frequency range was much higher, between 0 and 120 Hz. The shift in frequency between the off and the maximum electric field states was about 10 Hz which was significantly higher than that of other automotive ER engine mount, which is about 2-3 Hz. However, it is worth noting that the shift of 2-3 Hz happens with the operating frequency of 0–30 Hz. Thus, in both applications, engine mount and CD-ROM mount, the range of resonant frequency shifting is about 10% of the operating frequency.

4. Modeling the Response of the ER/MR Mounts

To predict the behavior of the ER/MR mounts before fabrication, a mathematical model has to be developed based on their physical structure. This model also helps to tune the mount parameters such that the mount response, stiffness, and damping characteristics are fit for a specific application. In general, the following assumptions are made prior to model development: the fluid is incompressible, the pressure in each chamber is uniform, and the mount is exposed only to vertical motion. In addition, it is considered that the top of the mount is excited harmonically by a known source (e.g., a shaker), and the bottom of the mount is fixed. Under these assumptions, the equations of motion were derived based on the procedure proposed by Hong et al. [16].

Accordingly, when the top rubber displaces, the flow of the ER/MR fluid through the flow passages is induced by the pressure difference between the upper and lower chambers. This pressure drop can be expressed by the linear momentum equation:

$$P_1 - P_2 = I_i \dot{Q}_i + R_i Q_i + \Delta P_{\mathrm{MR}}, \tag{1}$$

where P_1 is the pressure in the upper chamber, P_2 is the pressure in lower chamber of the mount, I_i is the fluid inertia, R_i is the fluid drag at zero magnetic field, Q_i is the fluid flow rate through the flow passage, and ΔP_{MR} is the pressure drop due to the yield stress of the MR fluid. The fluid pressure in upper and lower chambers can be calculated from the flow continuity equations [26]:

$$\dot{P}_1 = \frac{A_p}{C_1}\dot{x} - \frac{Q_i}{C_1}, \tag{2}$$

$$\dot{P}_2 = \frac{Q_i}{C_2}, \tag{3}$$

where C_1 and C_2 are the compliances of the upper and lower chambers, respectively, A_p is the piston area of the top rubber part, and $\dot{x}$ is the velocity of the top of the mount.

Assuming $Q_i = A_i \dot{x}_i$, where A_i is the cross sectional area of the flow passage and $\dot{x}_i$ is the fluid average velocity through the flow passage, substituting the integrations of (2) and (3) into (1) yields the following equation of motion for the fluid passing through the flow passage:

$$I_i A_i \ddot{x}_i + R_i A_i \dot{x}_i + A_i \left(\frac{1}{C_1} + \frac{1}{C_2}\right) x_i = \frac{A_P}{C_1} x + \Delta P_{\mathrm{MR}}, \tag{4}$$

where x is the displacement at the mount top. The pressure difference induced by the MR effect can be expressed as [27]

$$\Delta P_{\mathrm{MR}} = C\frac{L}{h}\tau_y(H)\,\mathrm{sign}\left(\dot{x}_i\right), \tag{5}$$

where C is a constant in the range of 2 to 3 depending on the steady-state flow conditions as suggested in Srinivasan and McFarland [27]. In this work, it is assumed that C is equal to 2, which corresponds to low-flow conditions. The other parameters appearing in (5) are as follows: L is the length inside the flow channel over which the magnetic field is applied, h is the distance between the magnetic poles, which is equal to the gap of the annular duct, b is the width of the channel, $\tau_y(H)$ is the MR fluid yield stress that is magnetic field (H) dependent. The cross section of the flow channel, that is, orifice, is approximated as a rectangle in this study with aforementioned dimensions b and h.

The hydraulic-related parameters are defined in Adiguna et al. [28]. Since the flow path is straight, the inertance of the fluid inside the flow passage is $I_i = \rho L/A_i$, where ρ is density of the MR fluid and L is the length of the flow passage. The fluid resistance within the flow passage is approximated based on the orifice geometry which is rectangular, $R_i = 128\eta L/\pi D_h^4$, where η is the MR fluid viscosity, which is shear rate dependent but assumed to be constant for this study; hydraulic diameter is $D_h = D_o - D_i = 2h$ for an annular duct.

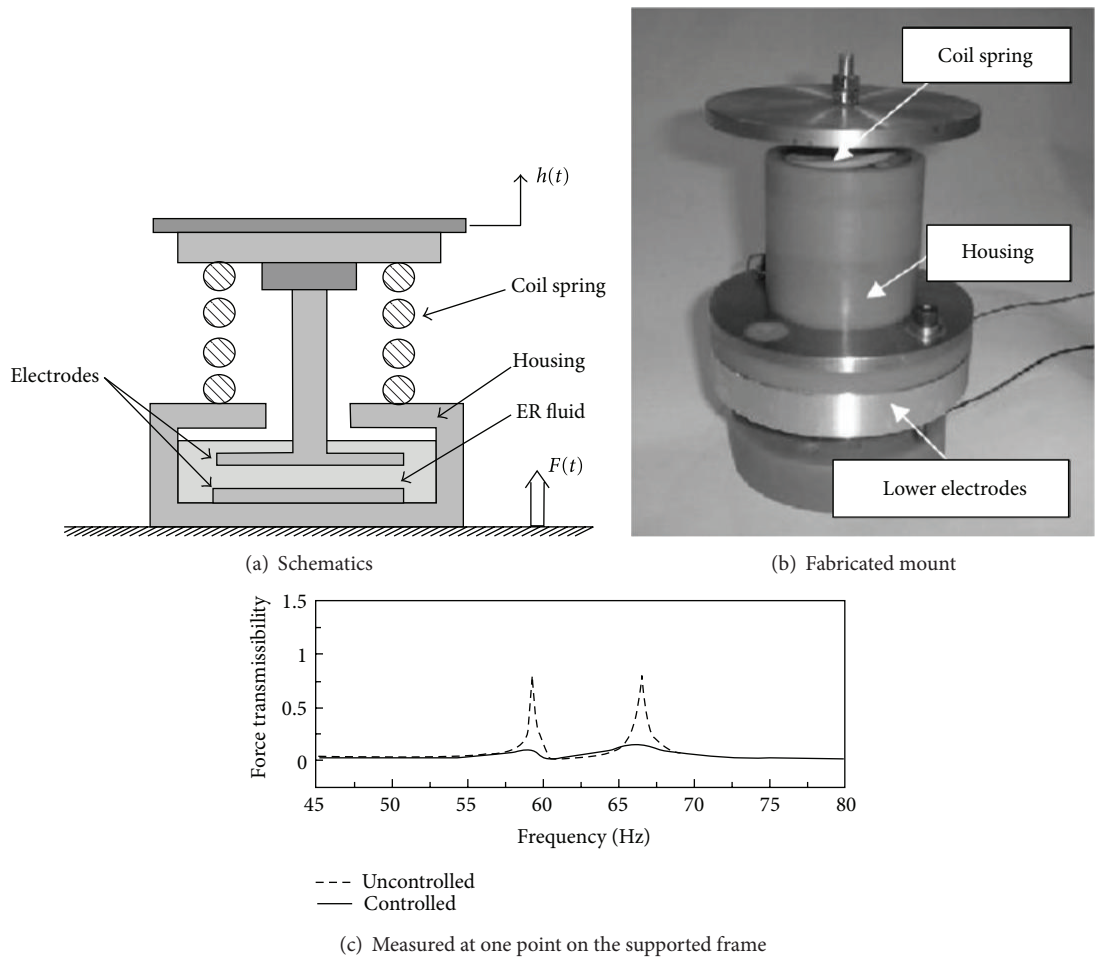

(a) Schematics (b) Fabricated mount

(c) Measured at one point on the supported frame

FIGURE 27: (a) Schematic of the squeeze mode ER mount developed by the Hong group; (b) actual prototype of the designed ER mount; (c) the controlled and uncontrolled force transmissibility of the mount as a function of the frequency of excitation [16].

The equation of motion pertaining to the squeeze mode is given by Hong et al. [16] as

$$M\ddot{x} + c_e\dot{x} + k_e x + C_{sq}\dot{x} + F_{sq} + A_p P_1 = F_{in}, \tag{6}$$

where F_{in} is the excitation force and c_e and k_e are the rubber damping and stiffness coefficients, respectively.

The damping constant associated with the viscous flow is

$$C_{sq} = \frac{3\pi R^3}{2(h_0 + x)^3}, \tag{6a}$$

and the damping force due to the fluid squeeze is

$$F_{sq} = \frac{3\pi R^3}{4(h_0 + x)}\tau(H)\,\mathrm{sign}(\dot{x}). \tag{6b}$$

The variables from the previous equations are as follows: h_0 is the gap between the parallel plates at the static deflection and R is the radii of the two plates. After substituting P_1 by (2) into (6), the final equation of motion can be written:

$$M\ddot{x} + c_e\dot{x} + \left(k_e + \frac{A_p^2}{C_1}\right)x + C_{sq}\dot{x} + F_{sq} = \frac{A_i A_p}{C_1}x_i + F_{in}. \tag{7}$$

5. Control of the MR/ER Mounts

Various control algorithms for MR/ER fluid-based devices have been researched and proposed so that these semi-active devices can achieve satisfactory performance for vibration isolation. The control algorithms investigated are described below and include linear quadratic Gaussian (LQG) control, groundhook control, skyhook control, fuzzy logic control, neural networks control, inversion-based control, integrator backstepping-based control, and hierarchical control. These control methods are either simple in design, such as skyhook control and fuzzy control, or more advanced, such as optimal control and neural networks control. These controllers

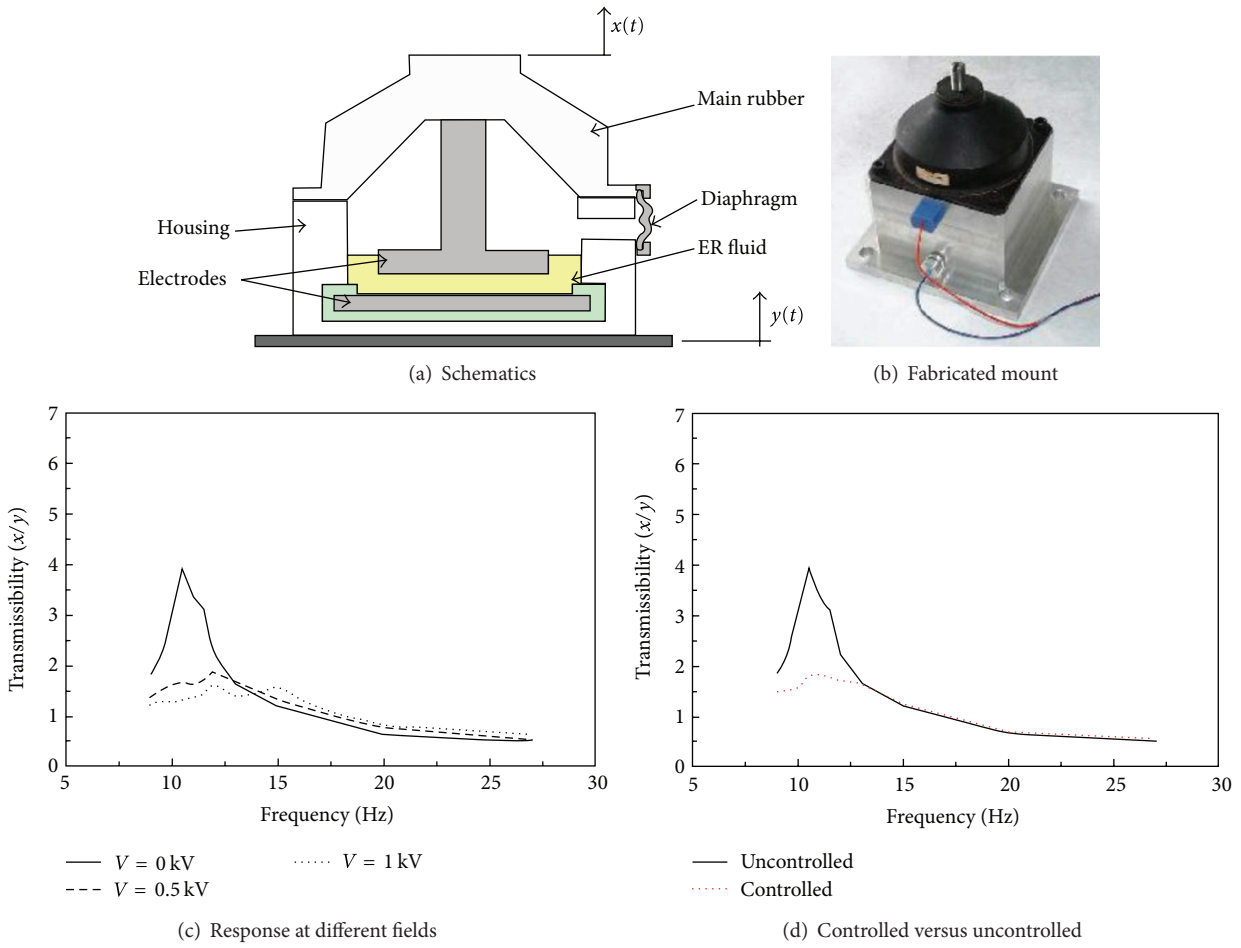

Figure 28: Squeeze mode ER mount by Hong et al. [22].

are used in different systems to achieve effective vibration isolation.

5.1. LQG Control. Hong and Choi [11] designed a linear quadratic Gaussian controller for a mixed mode, flow, and shear, MR fluid-based mount used to isolate the vibration of a structural system. Nondimensional formulation of the Bingham plastic flow model for the MR fluid was used in the control strategy. The structural system consists of a vibrating mass, semi-active MR fluid mount, and passive rubber mounts. The MR mount is installed as a semi-active isolator between the vibrating mass and the beam structure which is supported by two passive rubber mounts. The rubber element on the top of the MR mount supports the mass on the one hand and isolates the vibration transmission at the nonresonant frequency on the other hand. The governing equation is presented and rewritten in a state space model. The LQG controller is designed and experimentally verified as shown in

$$\dot{x}(t) = Ax(t) + Bu(t), \tag{8}$$

where $x(t)$ is the control state vector, A the control system matrix, B the control input matrix, and $u(t)$ the control input. The performance index chosen to be minimized is shown as follows:

$$J = \int_0^\infty \left\{x(t)^T Q x(t) + u(t)^T R u(t)\right\} dt, \tag{8a}$$

where Q is the state weighting semipositive matrix and R is the input weighting positive matrix. LQR is obtained as follows:

$$u(t) = -P^{-1}B^T x(t) = -Kx(t), \tag{8b}$$

where K is the state feedback gain matrix and P is the solution of an algebraic Riccati equation. For obtaining feedback signals, two accelerometers are attached on the vibrating mass and the flexible beam. The control voltage is calculated by LQG and applied to the MR mount via a digital-to-analog converter and a current supplier. The acceleration levels of the structural system are attenuated effectively by controlling the damping of the MR mount. The force transmission through the two rubber mounts is also suppressed by activating the MR mount. However, the results show that acceleration and force transmission with the LQG control are higher than the one without control at higher frequencies.

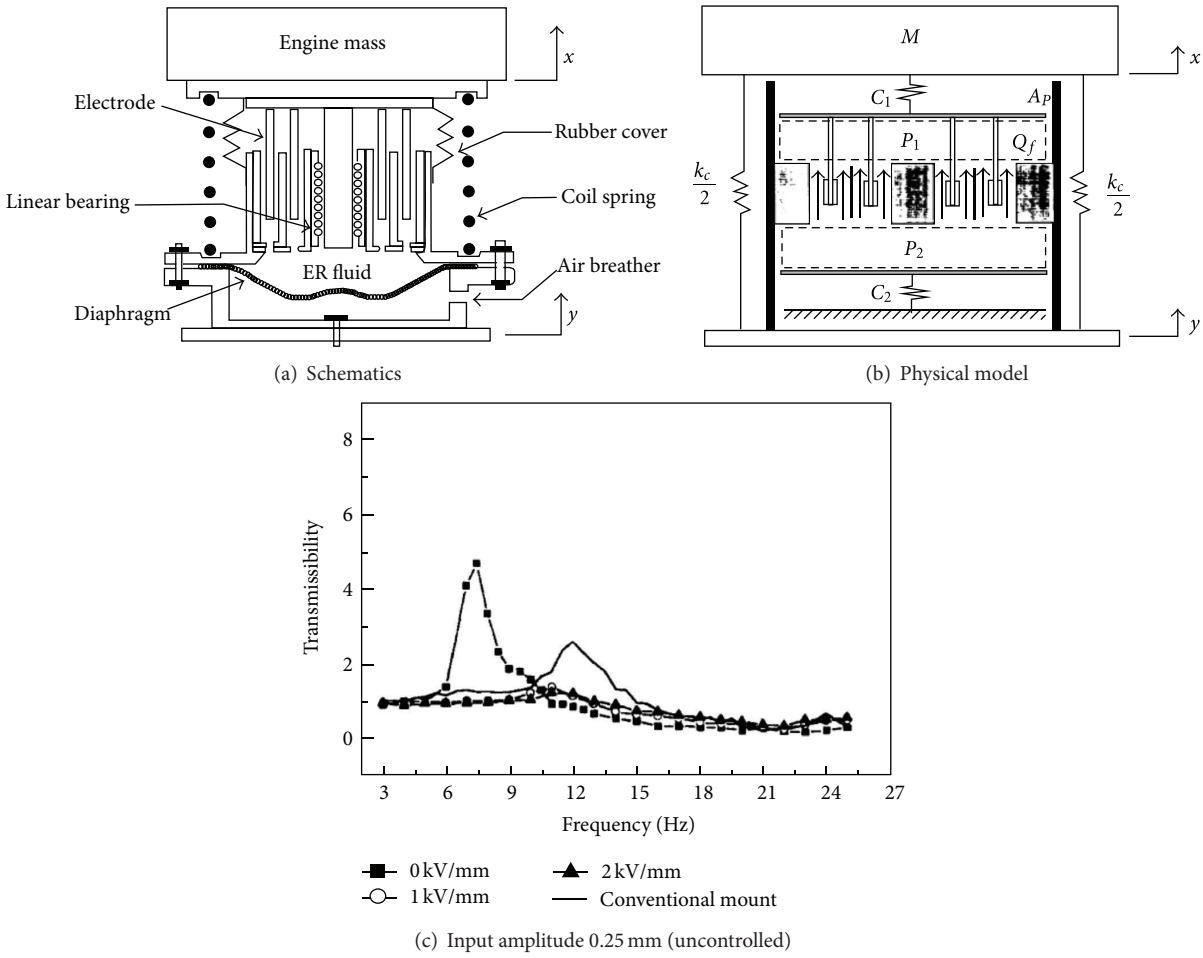

(a) Schematics (b) Physical model

(c) Input amplitude 0.25 mm (uncontrolled)

FIGURE 29: Mixed mode ER mount by Choi et al. [23].

5.2. On-Off Groundhook (On-Off DBG) Control. An on-off groundhook (on-off DBG) control based on displacement was proposed by Koo et al. [29] to effectively reduce the vibrations of a primary structure using an MR tuned vibration absorber. A tuned vibration absorber (TVA) is a vibratory subsystem attached to a primary system which consists of a mass, a spring, and a damper. TVAs are connected to the primary structure to offset its motion. A controllable MR damper changes a passive TVA into a semi-active TVA. The relative velocity is defined as the velocity of the structure mass minus the velocity of the TVA mass. The on-off DBG control provides two damping values which are identified as on state and off state damping; the adopted value is dependent on the product of the relative velocity across the damper and absolute displacement of the primary structure. When the relative velocity and the absolute displacement of the primary structure have the same direction, the on state damping value is used, and when they have the opposite direction, the off state damping value is chosen as shown in

$$\begin{aligned} x_1 v_{12} \geq 0, &\quad c_{\text{controllable}} = c_{\text{on}}, \\ x_1 v_{12} < 0, &\quad c_{\text{controllable}} = c_{\text{off}}. \end{aligned} \tag{9}$$

In (9), x_1 is the displacement of the structure and v_{12} is the relative velocity across the damper.

The test results demonstrate that different transmissibility curves are obtained when the MR mount is activated at different levels of input. The primary system alone has a resonant peak with a maximum transmissibility. Two resonant peaks appear when a TVA is added to the primary structure without activating the MR mount, simply because a degree of freedom was added to the system with the TVA. When the on state current is increased, it reduced the two resonant peaks while it increased the transmissibility between the two peaks. Continuing to increase the current makes the two peaks merge and increase in amplitude; this shows that the primary mass and the TVA mass are linked together. The unique resonant response is observed to be lower than that of the primary structure alone. The study showed that the controlled TVA outperformed a passive system, reducing the resonant peaks and providing good isolation around the structure's natural frequency.

5.3. Skyhook Control. Unsal et al. [30] developed a skyhook control system with the advantage of allowing selective

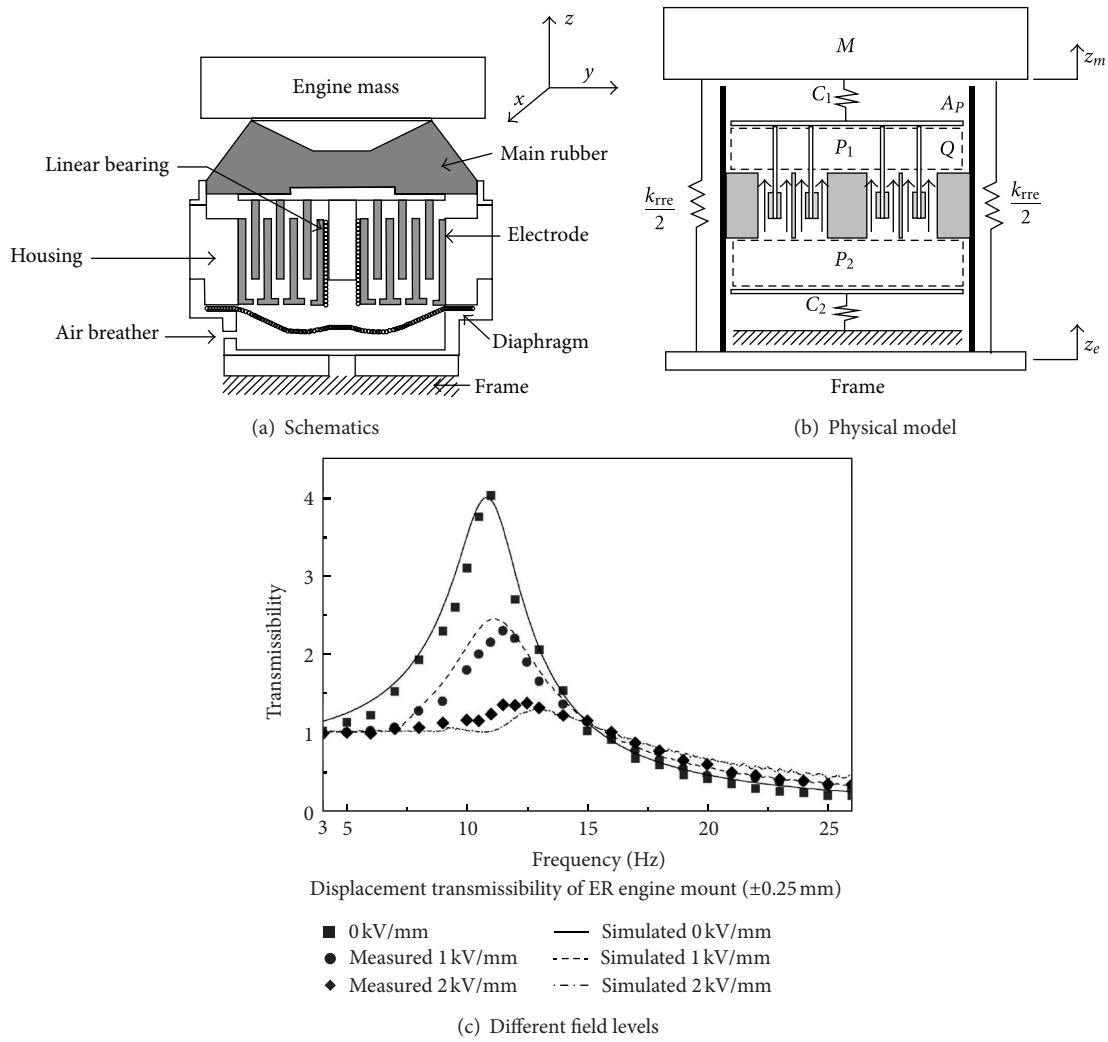

Figure 30: Mixed mode ER mount by Choi and Song [24].

energy dissipation for a model of a 6 DOF parallel platform. Each leg of the platform was modeled as a 2 DOF system and involved an MR damper, as illustrated in their paper. The Bingham plastic model was used and the relationships between the yield force and control current input, as well as the postyield damping coefficient and the control current input, were derived. The semi-active damper was developed to dissipate energy and was designed to apply an input current to the damper only under the condition that the relative velocity between the two bodies and the absolute velocity of the clean body are in the same direction. The control policy is described in

$$F = \begin{cases} F_{\max}, & \text{when } (\dot{x}_2 - \dot{x}_1)\,\dot{x}_2 > 0, \\ F_{\min}, & \text{when } (\dot{x}_2 - \dot{x}_1)\,\dot{x}_2 < 0, \end{cases} \tag{10}$$

where F is the damping coefficient, $\dot{x}_2$ is the absolute velocity of the clean body, and $\dot{x}_2 - \dot{x}_1$ is the relative velocity between two bodies. With the skyhook control method, the lowest transmissibility can be obtained for both 1 DOF and 2 DOF systems. The MR damper is either activated by applying a 2 A control input current or turned off by setting the current to zero. The control algorithm reduces the peak at the first resonant frequency and decreases the transmissibility at high frequencies for the 2 DOF. This made a good foundation for further extending the MR damper controlled 2 DOF to a 6 DOF parallel platform.

5.4. Fuzzy Skyhook/Groundhook Control. Ahmadian [31] developed a fuzzy skyhook/groundhook control for the semi-active MR system to improve the overall performance for the vehicle heave and roll motion during vehicle maneuvers. There are three steps of fuzzy logic control: fuzzification, rule evaluation, and defuzzification. In fuzzification, the vertical velocity of the axle, the relative velocity across the suspension, the absolute velocity of the vehicle body, and the acceleration of the vehicle body are chosen as four inputs and each input has its own membership functions. The damping value is chosen to be the output of the controller and has its own membership function. The rules of the system are developed for the inputs and the output. In defuzzification, the fuzzy

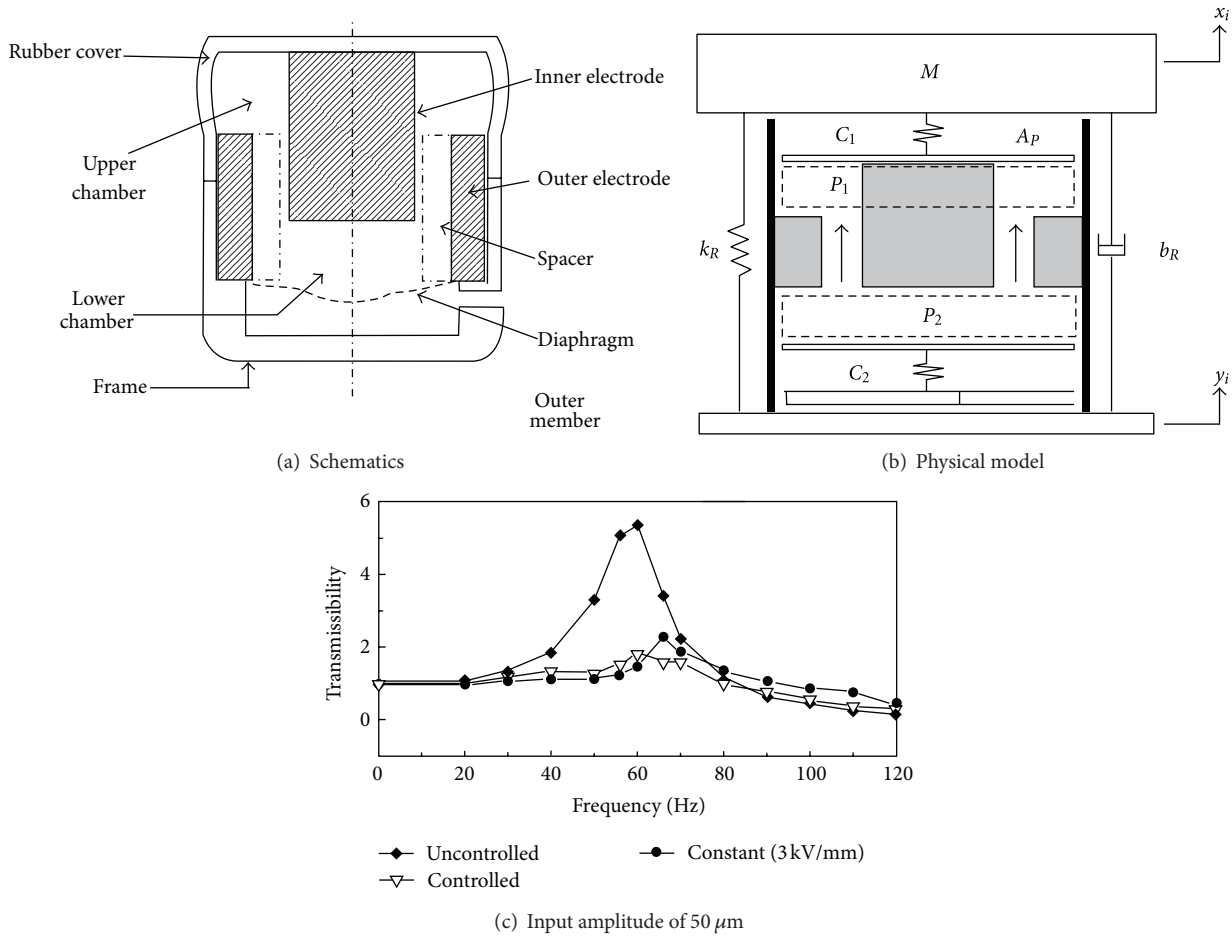

(a) Schematics (b) Physical model

(c) Input amplitude of 50 μm

FIGURE 31: Mixed mode ER mount by Lim et al. [25].

values are converted into a crisp value by the weighted average defuzzification method. The output is limited by its high and low state by comparing the output value with the ones of high and low state as shown in

$$c_{s,l} = \max\left\{\text{low state}, \min\left[c^*_{s,l}, \text{high state}\right]\right\}, \quad (11)$$

$$c_{s,r} = \max\left\{\text{low state}, \min\left[c^*_{s,r}, \text{high state}\right]\right\}. \quad (11a)$$

In the above equations, $c_{s,l}$ is the left controller crisp output, $c^*_{s,l}$ is the weighted average defuzzification method for left damper, $c_{s,r}$ is the right controller crisp output, and $c^*_{s,r}$ is the weighted average defuzzification method right damper. The results show that this fuzzy logic control for the semi-active suspensions could greatly reduce the vehicle heave and roll displacements, but increases the body acceleration peak value for road inputs at the tire, causing a less comfortable ride.

5.5. Neural Networks Control. Wang and Liao [35] presented the modeling and control of MR fluid dampers using neural networks. Based on the modified Bouc-Wen constitutive model for MR fluids, the inherent nonlinear behavior of the MR fluid was modeled in feedforward neural networks

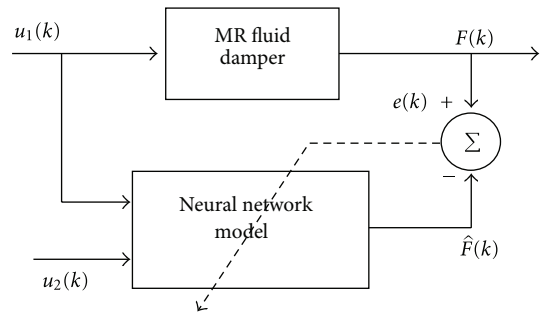

FIGURE 32: The identification for MR fluid damper by Wang et al. [32].

(FNN) and recurrent neural networks (RNN), in both, direct identification as shown in Figure 32 and inverse dynamics as shown in Figure 33. The results indicate that the direct identification dynamic model using RNN can predict the damping force accurately, and the inverse dynamic model using RNN can act as a damper controller to generate the command voltage for the MR fluid damper in semi-active mode. The simulation results are satisfactory and provide a new method for the MR fluid damper controller. However,

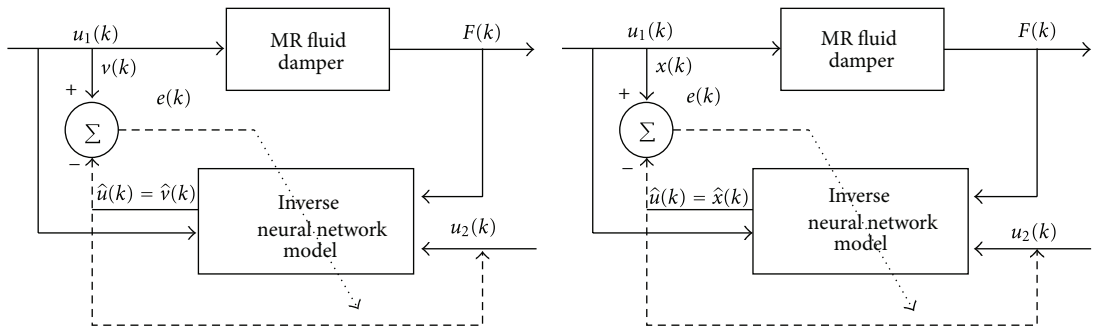

(a) Force to command voltage model (b) Force to displacement model

Figure 33: Inverse modeling for the MR damper using neural network by Wang et al. [32].

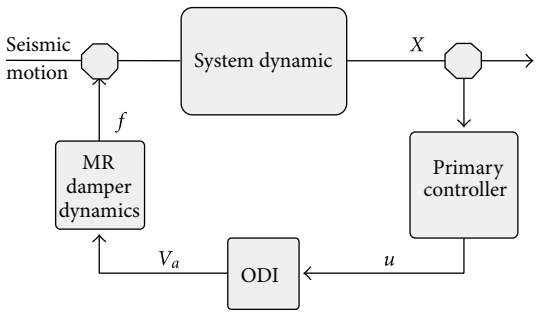

Figure 34: Schematic diagram of a dynamic inversion controller by Ali and Ramaswamy [33].

this controller requires training; the training data needs to cover most situations occurring in practical applications and needs to be simple, in order to speed up the training process. Furthermore, the neural networks control works like a "black box" as the process of generating the outcome is not explicitly stated.

5.6. Hybrid Structural Control. Ali and Ramaswamy [33] used the RD-1005-3 MR damper developed by Lord Corporation for their study of a base isolation system in a three-story building. A single MR damper is connected at the base of the building. The Bouc-Wen model is used, and dynamic inversion-based control and integrator backstepping-based control are stated and compared with clipped optimal control, optimal fuzzy logic control. Clipped optimal control makes the control force suboptimal when it changes the voltage of MR damper from zero to its maximum value. From the results, the dynamic inversion-based control, shown in Figure 34, and integrator backstepping-based control, shown in Figure 35, are better than clipped optimal control and genetic algorithm-based fuzzy logic control because the latter two controllers decreased the isolator displacement at the cost of an increase in superstructure acceleration, while the former two controllers provide a tradeoff between isolator displacement and superstructure acceleration. They are able to monitor the voltage needed to control the structural vibration taking into account the effect of the supplied and commanded voltage dynamics of the damper.

5.7. Hierarchical Control. Wang et al. [34] designed a control system for the mixed-mode MR fluid mount. Based on a model for a uniaxial MR mount, a controller has been designed to achieve the lowest possible vibration transmissibility. Furthermore, the MR mount in two degrees of freedom structure has been modeled. Displacement transmissibility and force transmissibility are considered in this scenario, with the goal of minimizing both. The controllers to achieve the lowest value for each type of transmissibility were designed. Moreover, a hierarchical controller for realizing the tradeoff between these two types of transmissibility was also constructed as shown in Figure 36. At last, a fuzzy logic controller is devised to closely reproduce the effect of the hierarchical controller. The experiments are set up to realize the hardware-in-the-loop tests. Results from the experiments show that the mixed-mode MR fluid mount is able to achieve desired dynamic stiffness which is directly related to vibration transmissibility. This study provided a fundamental understanding on the behavior of MR fluid mount in a single degree of freedom model and two degrees of freedom model. The significantly reduced transmissibility demonstrates effectiveness of the designed control system. The results of this research provide insight into the development of the control system for other effective isolation devices.

6. Conclusions

This paper presents a review of all relevant papers known to the authors describing design, modeling, and control of electrorheological- and magnetorheological-based mounts. The material presented here indicates that substituting regular hydraulic fluid with ER or MR fluids can lead to a successful development of semiactive mounts. These types of mounts are desirable as they allow real time changes on the dynamic stiffness of the mount, shifting of the notch, and peak frequencies of the mount over a fairly wide range of frequencies. Such response is desired as new technologies, for example, engine on demand and pneumatic or hydraulic

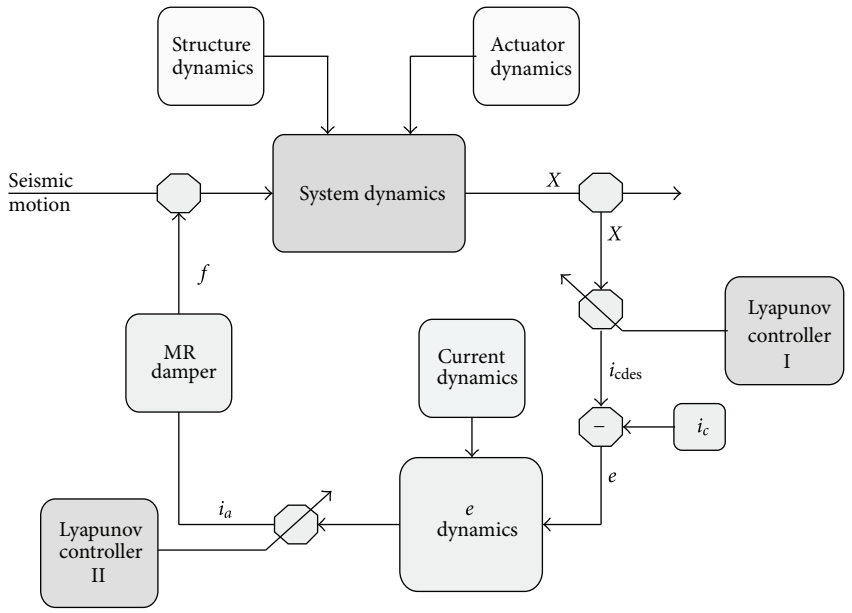

FIGURE 35: Schematic diagram of integral backstepping-based monitoring by Ali and Ramaswamy [33].

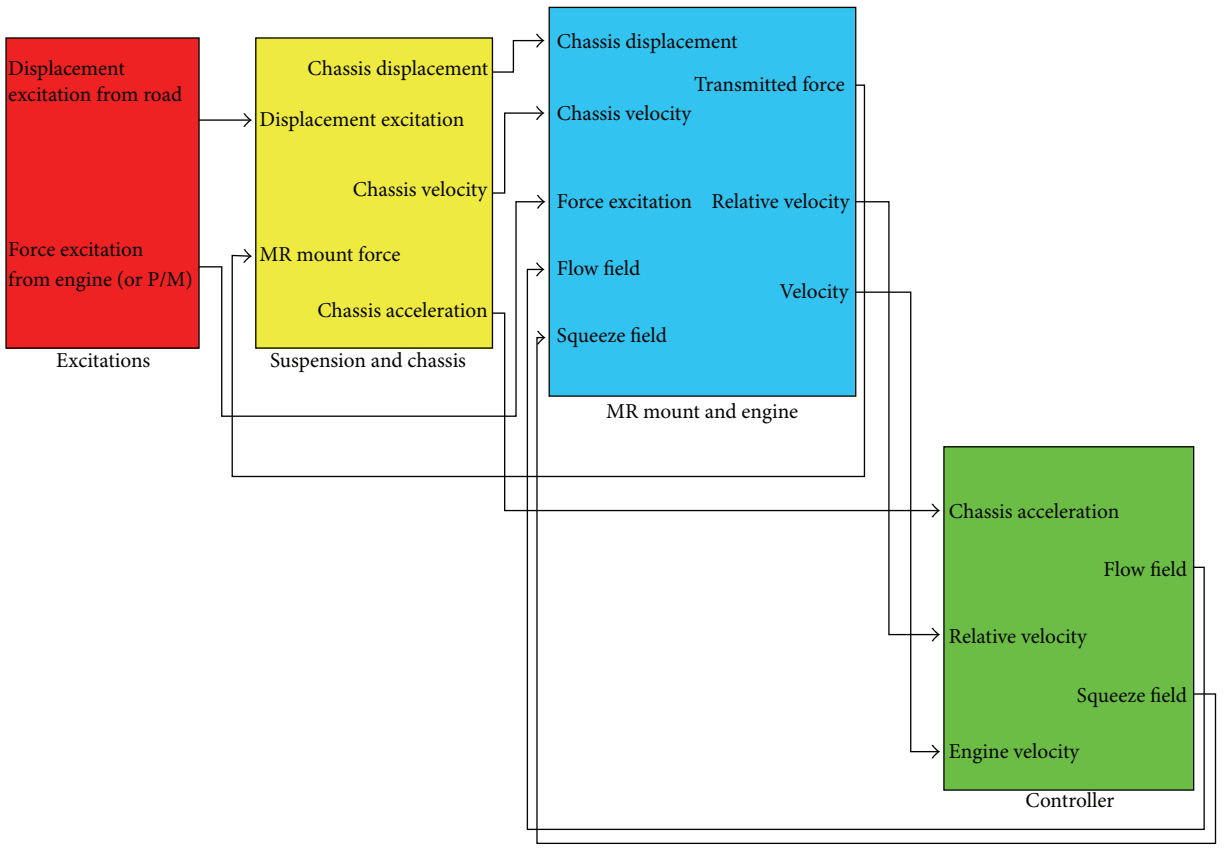

FIGURE 36: Model of hierarchical control of the MR mount in TDOF by Wang et al. [34].

actuation, induce vibrations to the chassis over a wider range of amplitudes and frequencies. Optimal operation of MR and ER semi-active mounts requires a suitable control strategy which seems to elude the engineering community. Further research in the control area is needed to increase the potential of these mounts being adopted in more engineering applications.

References

[1] J. DeCicco and F. Fung, "Global warming on the road—the climate impact of America's automobiles," http://www.edf.org/documents/5301_Globalwarmingontheroad.pdf.

[2] K. Kumagai, M. Fujiwara, M. Segawa, R. Sato, and Y. Tamura, "Development of a 6-cylinder gasoline engine with new variable cylinder management technology," in *Proceedings of the SAE World Congress and Exhibition*, April 2008, paper no. 2008-01-0610.

[3] L. V. Pérez, G. R. Bossio, D. Moitre, and G. O. García, "Optimization of power management in an hybrid electric vehicle using dynamic programming," *Mathematics and Computers in Simulation*, vol. 73, no. 1–4, pp. 244–254, 2006.

[4] Y. Ito, S. Tomura, and S. Sasaki, "Development of vibration reduction motor control for hybrid vehicles," in *Proceedings of the 33rd Annual Conference of the IEEE Industrial Electronics Society (IECON '07)*, pp. 516–521, November 2007.

[5] Y. K. Ahn, M. Ahmadian, and S. Morishita, "On the design and development of a Magneto-Rheological mount," *Vehicle System Dynamics*, vol. 32, no. 2, pp. 199–216, 1999.

[6] M. Abuhaiba, *Mathematical modeling and analysis of a variable displacement hydraulic bent axis pump linked to high pressure and low pressure accumulators [Ph.D. Dissertation]*, Mechanical, Industrial and Manufacturing Department, University of Toledo, 2009.

[7] A. Agrawal, C. Ciocanel, T. Martinez et al., "A bearing application using magnetorheological fluids," *Journal of Intelligent Material Systems and Structures*, vol. 13, no. 10, pp. 667–673, 2002.

[8] J. D. Carlson and M. R. Jolly, "MR fluid, foam and elastomer devices," *Mechatronics*, vol. 10, no. 4, pp. 555–569, 2000.

[9] R. Ay, M. F. Golnaraghi, and A. Khajepour, "Investigation on a semi-active hydro mount using Mr Fluid," in *Proceedings of the NATO, Symposium on Active Control Technology for Enhanced Performance Operational Capabilities of Military Aircraft, Land Vehicles and Sea Vehicles*, Braunschweig, Germany, May 2000.

[10] Y. K. Ahn, B. S. Yang, M. Ahmadian, and S. Morishita, "A small sized variable-damping mount using magneto-rheological fluid," *Journal of Intelligent Material Systems and Structures*, vol. 16, no. 2, pp. 127–133, 2005.

[11] S. R. Hong and S. B. Choi, "Vibration control of a structural system using magneto-rheological fluid mount," *Journal of Intelligent Material Systems and Structures*, vol. 16, no. 11-12, pp. 931–936, 2005.

[12] Delphi Corp., *Delphi Magneto-Rheological (MR) Powertrain Mount*, 2005.

[13] D. E. Barber and J. D. Carlson, "Performance characteristics of prototype MR engine mounts containing LORD glycol MR fluids," in *Proceedings of the 11th International Conference on Electrorheological Fluids and Magnetorheological Suspensions*, Dresden, Germany, 2009.

[14] H. Mansour, S. Arzanpour, M. F. Golnaraghi, and A. M. Parameswaran, "Semi-active engine mount design using auxiliary magneto-rheological fluid compliance chamber," *Vehicle System Dynamics*, vol. 49, no. 3, pp. 449–462, 2011.

[15] T. Nguyen, *A novel semi-active magnetorheological mount for vibration isolation [Dissertation]*, 2009.

[16] S. R. Hong, S. B. Choi, W. J. Jung, and W. B. Jeong, "Vibration isolation of structural systems using squeeze mode ER mounts," *Journal of Intelligent Material Systems and Structures*, vol. 13, no. 7-8, pp. 421–424, 2002.

[17] R. Stanway, J. L. Sproston, M. J. Prendergast, J. R. Case, and C. E. Wilne, "ER fluids in the squeeze-flow mode: an application to vibration isolation," *Journal of Electrostatics*, vol. 28, no. 1, pp. 89–94, 1992.

[18] E. W. Williams, S. G. Rigby, J. L. Sproston, and R. Stanway, "Electrorheological fluids applied to an automotive engine mount," *Journal of Non-Newtonian Fluid Mechanics*, vol. 47, pp. 221–238, 1993.

[19] J. L. Sproston, R. Stanway, M. J. Prendergast, J. R. Case, and C. E. Wilne, "Prototype automotive engine mount using electrorheological fluids," *Journal of Intelligent Material Systems and Structures*, vol. 4, no. 3, pp. 418–419, 1993.

[20] J. L. Sproston, R. Stanway, E. W. Williams, and S. Rigby, "The electrorheological automotive engine mount," *Journal of Electrostatics*, vol. 32, no. 3, pp. 253–259, 1994.

[21] W. J. Jung, W. B. Jeong, S. R. Hong, and S. B. Choi, "Vibration control of a flexible beam structure using squeeze-mode ER mount," *Journal of Sound and Vibration*, vol. 273, no. 1-2, pp. 185–199, 2004.

[22] S. R. Hong, S. B. Choi, and D. Y. Lee, "Comparison of vibration control performance between flow and squeeze mode ER mounts: experimental work," *Journal of Sound and Vibration*, vol. 291, no. 3–5, pp. 740–748, 2006.

[23] S. B. Choi, Y. T. Choi, C. C. Cheong, and Y. S. Jeon, "Performance evaluation of a mixed mode ER engine mount via hardware-in-the-loop simulation," *Journal of Intelligent Material Systems and Structures*, vol. 10, no. 8, pp. 671–677, 1999.

[24] S. B. Choi and H. J. Song, "Vibration control of a passenger vehicle utilizing a semi-active ER engine mount," *Vehicle System Dynamics*, vol. 37, no. 3, pp. 193–216, 2002.

[25] S. C. Lim, J. S. Park, S. B. Choi, and Y. P. Park, "Vibration control of a CD-ROM feeding system using electro-rheological mounts," *Journal of Intelligent Material Systems and Structures*, vol. 12, no. 9, pp. 629–637, 2001.

[26] R. I. Woods and K. L. Lawrence, *Modeling and Simulation of Dynamic Systems*, Prentice Hall, London, UK, 1997.

[27] A. V. Srinivasan and M. D. McFarland, *Smart Structures: Analysis and Design*, Cambridge University Press, New York, NY, USA, 2001.

[28] H. Adiguna, M. Tiwari, R. Singh, H. E. Tseng, and D. Hrovat, "Transient response of a hydraulic engine mount," *Journal of Sound and Vibration*, vol. 268, no. 2, pp. 217–248, 2003.

[29] J. H. Koo, M. Ahmadian, and M. Elahinia, "Semi-active controller dynamics in a magneto-rheological tuned vibration absorber," in *Smart Structures and Materials: Damping and Isolation*, vol. 5760 of *Proceedings of SPIE*, pp. 69–76, March 2005.

[30] M. Unsal, C. Niezrecki, and C. D. Crane :, "Six DOF vibration control using magnetorheological technology," in *Symposium on Smart Structures and Materials*, Proceedings of SPIE, San Diego, Calif, USA, February 2006.

[31] M. Ahmadian, "On the development of fuzzy skyhook control for semiactive magneto rheological systems," in *Smart Structures and Materials: Damping and Isolation*, vol. 5760 of *Proceedings of SPIE*, pp. 268–282, March 2005.

[32] X. Wang, F. Gordaninejad, and G. Hitchcock, "A magneto-rheological fluid-elastomer vibration isolator," in *Smart Structures and Materials: Damping and Isolation*, vol. 5760 of *Proceedings of SPIE*, pp. 217–225, March 2005.

[33] S. F. Ali and A. Ramaswamy, "Hybrid structural control using magnetorheological dampers for baseisolated structures," *Smart Materials and Structures*, vol. 18, no. 5, Article ID 055011, 2009.

[34] S. . Wang, M. Elahinia, and T. Nguyen, "Displacement and force control of a quarter car usinga mixed mode MR mount," *Shock and Vibration*. In press.

[35] D. H. Wang and W. H. Liao, "Modeling and control of magnetorheological fluid dampers using neural networks," *Smart Materials and Structures*, vol. 14, no. 1, pp. 111–126, 2005.